Interaction of Wedge-Shaped Proteins in Flat Bilayer Membranes

ARTICLE *in* THE JOURNAL OF PHYSICAL CHEMISTRY B · AUGUST 1998

Impact Factor: 3.3 · DOI: 10.1021/jp9807266

2 AUTHORS:

Tomàs Sintes
University of the Balearic Islands
45 PUBLICATIONS **629** CITATIONS
SEE PROFILE

A. Baumgaertner
University of Duisburg-Essen
113 PUBLICATIONS **2,070** CITATIONS
SEE PROFILE

Interaction of Wedge-Shaped Proteins in Flat Bilayer Membranes

T. Sintes and A. Baumgaertner*

Forum Modellierung, Forschungszentrum, 52425 Jülich, Germany

Received: January 8, 1998; In Final Form: March 12, 1998

We present extensively Monte-Carlo simulations of two conically-shaped proteins in parallel and antiparallel relative orientation, embedded in a flat lipid bilayer membrane with zero bending elasticity. We found two protein attractive regimes. The first one, in the range $r_s < \sigma_L$, where σ_L is the lipid diameter and r_s the distance between the surfaces of the two proteins, is due to depletion effects. The second one, in the range $1 < r_s/\sigma_L < 6$, originates from the density and orientational fluctuations of the lipids around each protein. It is found that the attractive force decays exponentially with a correlation length $\xi/\sigma_L \approx 3.2$ independent of the shape and the size of the proteins.

I. Introduction

Cell membranes are a highly heterogeneous mixture of lipids and inhomogeneities like proteins and cholesterols. In many biological membranes, proteins may cover almost 50% of the surface area, so that proteins are separated by a few layers of lipids and tend to pack even in the absence of cytoskeleton interactions. Lipid−protein interactions play therefore a crucial role in the clustering process and thus, in the control of membrane functionality[1,2] and structure. It may modulate the activity of membrane-bound enzymes[3] or lateral distribution of proteins on the membrane surface.[4]

Several mechanisms have been proposed to explain the aggregation process. Direct interactions between inclusions due to Van der Waals and electromagnetic forces are well understood.[5] They are important, for example, at temperature driven phase separations among lipids and proteins[6] or between dipoles on pairs of antiparallel α-helices.[7] Indirect interactions that are membrane-induced by imposed perturbations on the bilayer structure, have been also largely considered. Local curvature effects and membrane undulations are predicted to lead to long-range interactions of $1/R^4$ type.[8−13] At short distances, of the order of a few lipid layers between two proteins, a nonspecific lipid-mediated attraction may exist[14−17] that is shown to decay exponentially. In addition, the aggregation of proteins can also be related to the presence of asymmetric proteins or to asymmetric properties of curved membranes.[18]

In general, amphiphilic monolayers have a spontaneous curvature. In bilayers, the tendency to curve is balanced and it adopts, locally, a flat configuration. However, the presence of inclusions is shown in one-dimension[19] to decouple the two monolayers. As a consequence, the spontaneous curvature may dominate the perturbation profile and the interaction between inclusions depends on the magnitude of the spontaneous curvature and the inclusion boundary condition. For symmetric inclusions the force is found to be attractive, but for inclusions that are asymmetric under reflection in the plane of the membrane the character of the force may depend on the temperature and bending energies.[9−11]

A different situation corresponds to a bilayer composed of amphiphiles with zero spontaneous curvature or when the stretching dominates the bending energy in the limit of infinite rigidity. Under such conditions one expects that the presence of conical inclusions may affect the local fluctuation of lipids and, thus, the range and sign of the interaction at short distances.

Here we present a detailed Monte Carlo simulation of two conically shaped proteins embedded in a lipid bilayer membrane. We have estimated the forces and the range of interaction for proteins being in a parallel or antiparallel relative orientation. In both cases we found two types of lipid-mediated attractive forces. The first one, limited to the depletion zone around the proteins, $r < \sigma_L$, where σ_L is the thickness of the lipid molecule, can be described in terms of the Asakura−Oosawa approach.[20] The second type is induced by density and orientational fluctuations of the lipids around a protein. The range of this fluctuation-induced attraction seems to decay exponentially, although the range of attraction is rather large and in the order of $1.5 < r/\sigma_L < 6$. The result in this regime has been compared with previous studies[21] with cylindrical type inclusions and different diameter sizes obtaining the same behavior.

II. Model Membrane

We have used Monte Carlo methodes to investigate a model lipid-bilayer membrane at air−water interface[23] containing two conically shaped model proteins. Two cases have been considered: the proteins being in a parallel or antiparallel orientation with respect to each other (see Figure 1). In both cases, we have introduced an assembly of lipids per layer such that we have an equal density in each layer. Periodic boundary conditions in the $x-y$ plane have been applied. The total number of lipids in both layers is $N_L \approx 1000$. The actual number of lipids in each layer, however, depends slightly on the shapes and the mutual orientation of the conical proteins. A lipid molecule has been modelled by a flexible chain of $M = 5$ effective monomers of diameter $\sigma_L = 4$ Å. The proteins, whose axes are oriented perpendicularly to the $x-y$ plane, have a maximum diameter of $\sigma_P = 16$ Å and a minimum of σ_L (Figure 1). The size of the cell is chosen to be $L^2 = 22500$ Å^2. Finite size effects for the equilibrium properties of the membrane are negligible.

In this coarse-grained representation of the lipid molecule, each monomer represents a group of about 3 or 4 successive chemical monomers (CH_2 groups) of a real lipid molecule.[24]

* To whom correspondence should be addressed. Forum Modellierung (MOD), Forschungszentrum Juelich, 52425 Juelich, Germany. www: http:/www.kfa-juelich.de/mod.

S1089-5647(98)00726-3 CCC: $15.00
Published on Web 08/19/1998

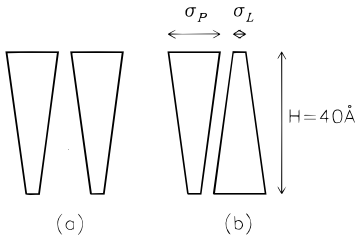

Figure 1. Schematic representation of the wedge-shaped protein configurations: (a) parallel, (b) antiparallel.

The distribution of the angle between subsequent effective bonds can be modeled by a suitable effective potential for bond angles, and the correct persistence length of the chains can be, at least, reproduced roughly. Thus, effective intramolecular potentials are introduced to take into account chain connectivity and chain stiffness. Because of the coarse-grained modeling of the chain we neglect to introduce torsional potentials.

The total energy of the lipids contain the following contributions:

$$U = U_{\text{bond}} + U_{\text{angle}} + U_{\text{steric}} \tag{1}$$

Commonly used potentials and parameters for U have been taken from previous Monte Carlo simulations.[25,26] The vibrational energy of the bonds along the chain backbone is

$$U_{\text{bond}} = \sum_{\text{bonds}} \epsilon_b (b/b_0 - 1)^2 \tag{2}$$

where $\epsilon_b = 250$ kcal/mol and $b_0 = 3.9$ Å. We use an upper and lower bond for the extension of the spring such that $U_{\text{bond}}(b > b_{\max}) = U_{\text{bond}}(b < b_{\min}) = \infty$, where $b_{\min} = 3.6$ Å, $b_{\max} = 4.2$ Å. The bending energy between neighboring bonds is

$$U_{\text{angle}} = \sum_{\text{angles}} \epsilon_\theta (1 + \cos\theta)^2 \tag{3}$$

where $\epsilon_\theta = 15$ kcal/mol. The last term represents the steric interactions among the monomers of the lipids,

$$U_{\text{steric}} = \sum_{i,j=1}^{M \times N_L} V(r_{ij}) \tag{4}$$

where V is a hard sphere potential

$$V(r_{ij}) = \begin{cases} 0 & \text{for } |\mathbf{r}_i - \mathbf{r}_j| > \sigma \\ \infty & \text{for } |\mathbf{r}_i - \mathbf{r}_j| < \sigma \end{cases} \tag{5}$$

and $\sigma = \sigma_L$ was employed for intermolecular interactions and for interactions between monomers that are separated by more than one bond in the same molecule. Similarly, the steric interactions between the monomers of the lipids and the proteins have been taken into account by the same hard core potential, but then $\sigma = (\sigma_h(z) + \sigma_L)/2$, $\sigma_h(z)$ being the protein diameter at height z.

Since specific interactions between water and lipid heads are not included, stability of the structure of this model membrane is provided by introducing two fixed interfaces to which the lipid head groups are tethered. Such interfaces are modeled by two impenetrable surfaces located at $z = 40$ Å and $z = 0$ Å for the upper and lower layer, respectively. Each tether is modeled for simplicity by an athermal potential $U(z)$, where $U(z) = 0$ for $0 < z < \sigma_L$ and $40 > z > (40 - \sigma_L)$, and $U(z) = \infty$ otherwise. Thus, lipid heads are bound but can diffuse in close proximity to the interfaces. The separation of 40 Å between the two interfaces has been chosen with regard to usual experimental situations and with regard to minimize the steric repulsion between the two leaflets of the bilayer.

III. Simulation Details

The numerical implementation of the algorithm follows a Metropolis scheme. A lipid or protein is randomly selected at each trial and is attempted to move from its original position. If a protein is selected, a translation in the $x-y$ plane is proposed. If a lipid is chosen, its dynamics is performed by randomly displacing a selected bead from the chain. Each move is accepted if

$$\exp(-\Delta U/RT) > \eta \tag{6}$$

where $0 < \eta < 1$ is a random number and ΔU is the difference between the old and the new energy of the system. Throughout the simulations we used a temperature of $T = 305$ K and hence $RT = 0.606$ kcal/mol. One Monte Carlo step (MCS) corresponds to $[(MN_L) + 2]$ trials and defines the unit time. The maximum size of the proposed movement is adjusted to reach an acceptance rate of at least 50%. A link-cell method[27] has been implemented in the algorithm to efficiently check ΔU.

The simulations start by placing the two wedge-shaped proteins at a distance R. The initial lipid configuration is at random. The system is equilibrated at constant volume for 10^5 MCS keeping the proteins fixed. The mean area per lipid is approximately of 46 Å^2, and the average orientation of the lipids respect to the surface normal is $\langle\cos(\theta)\rangle = 0.83$. Both quantities are comparable to experimental values.[28]

A. Computing the Forces. To compute the forces between proteins, we have used an extension of a numerical technique, originally applied to colloidal dispersions in nonadsorbing polymer solutions,[29] which also has been succesfully applied to the case of interacting polymer brushes.[30] We briefly review here this latter algorithm.

The main idea consists in computing the change in the free energy F due to an infinitesimal change in the relative positions of the interacting colloids. The force, in units of k_BT is given by

$$f(R) \equiv \frac{F}{k_B T} = \frac{\partial \ln Z(R)}{\partial R} \tag{7}$$

where $Z(R)$ is the partition function of the system that represents all possible lipid configurations compatible with the presence of the wedge-shaped inclusions separated a distance R. $f(R) > 0$ corresponds to a repulsive force directed along the line joining the inclusions.

Let $\Omega_C(R) \subset Z(R)$ be the subset of configurations compatible with a movement of one of the inclusions toward the other by an amount δR. Similarly, let $\Omega_E(R - \delta R) \subset Z(R - \delta R)$ be the set of configurations of $Z(R - \delta R)$ in which it is possible to shift the inclusions a distance δR apart without overlapping a lipid. The compresion probability is just $P_C(R) = \Omega_C(R)/Z(R)$, and the probability that the expansion can be done is $P_E(R - \delta R) = \Omega_E(R - \delta R)/Z(R - \delta R)$. Since the subsets $\Omega_C(R)$ and $\Omega_E(R - \delta R)$ are in one-to-one correspondence, we have

$$\frac{Z(R)}{Z(R - \delta R)} = \frac{P_E(R - \delta R)}{P_C(R)} \tag{8}$$

The expansion and compresion probabilities are obtained through the evaluation of the density pair-correlation function $g_{ij}(r,\theta)$. Thus, $g_{ij}(r,\theta)\mathrm{d}r\,\mathrm{d}\theta$ is the probability of finding a protein

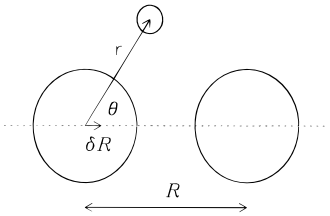

Figure 2. Representation of a virtual compresion in the direction joining the proteins with the presence of a lipid monomer.

i and a lipid monomer j within a distance, projected on the $x-y$ plane, (r, $r + \mathrm{d}r$) and an angle (θ, $\theta + \mathrm{d}\theta$), measured respect to the line that join the two inclusions (see Figure 2). After compresion, particles i and j may overlap if $r^2 + (\delta R)^2 - 2r\delta R \cos\theta < \sigma^2$. In the limit $\delta R \rightarrow 0$, the overlap condition becomes $r < \sigma + \delta R \cos\theta$. Therefore, the probability per MCS that a compresion is not allowed is given by

$$\overline{P_{\mathrm{C}}}(i,j) = \int_{-\pi/2}^{\pi/2}\int_{\sigma}^{\sigma+\delta R\cos\theta} g_{ij}(r,\theta)\mathrm{d}r\,\mathrm{d}\theta \tag{9}$$

$$\approx \delta R\int_{-\pi/2}^{\pi/2} g_{ij}(\sigma,\theta)\cos\theta\mathrm{d}\theta \tag{10}$$

and the compresion probability can be obtained as

$$P_{\mathrm{C}}(R) = \prod_{i=1}^{2}\prod_{j=1}^{MN_L}[1 - \overline{P_{\mathrm{C}}}(i,j)] \tag{11}$$

In the approximation $\delta R \rightarrow 0$ we have

$$\frac{\partial \ln Z(R)}{\partial R} \approx \frac{1}{\delta R}\ln\frac{Z(R)}{Z(R-\delta R)} \tag{12}$$

and taking the logarithm in eq 11 expanded up to order δR,

$$\ln(P_{\mathrm{C}}(R)) = -\delta R\int_{-\pi/2}^{\pi/2}\sum_{i=1}^{2}\sum_{j=1}^{MN_L} g_{ij}(\sigma,\theta)\cos\theta\mathrm{d}\theta \tag{13}$$

By defining

$$G(\sigma,\theta) = \sum_{i=1}^{2}\sum_{j=1}^{MN_L} g_{ij}(\sigma,\theta) \tag{14}$$

we can rewrite eq 13 as

$$\ln(P_{\mathrm{C}}(R)) = -\delta R\int_{-\pi/2}^{\pi/2} G(\sigma,\theta)\cos\theta\,\mathrm{d}\theta \tag{15}$$

where $G(r,\theta)\mathrm{d}r\ \mathrm{d}\theta$ represents the averaged density of lipid monomers, projected on the $x-y$ plane, separated a distance (r, $r + \mathrm{d}r$) from a protein, within an angle in the interval (θ, $\theta + \mathrm{d}\theta$).

In the same way, the expansion probability is given by

$$\ln(P_{\mathrm{E}}(R-\delta R)) = -\delta R\int_{\pi/2}^{-\pi/2} G(\sigma,\theta)\cos(\pi-\theta)\,\mathrm{d}\theta \tag{16}$$

Introducing previous expressions in eqs 8 and 12, the force is given by

$$f(R) = \int_0^{2\pi} G(\sigma,\theta)\cos\theta\,\mathrm{d}\theta \tag{17}$$

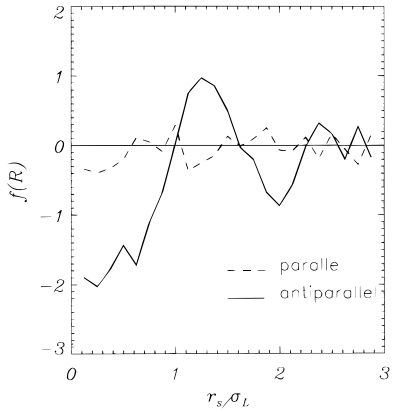

Figure 3. Force $f(R)$ versus distance r_s/σ_{L} for the parallel and antiparallel protein configuration.

Numerically the above integral has been replaced by the averaged sum

$$\tilde{f}(r) = \left\langle \frac{1}{2\pi r\Delta r}\sum_{i=1}^{2}\sum_{j,r<r_{ij}<r+\Delta r}^{MN_L}\cos\theta_{ij} \right\rangle \tag{18}$$

so that,

$$f(R) = \tilde{f}(r \rightarrow \sigma) \tag{19}$$

In the simulation we have considered $\Delta r = 0.01$. Different values of R have been chosen, such that the closest distance between the surfaces of the proteins varies between $r_{\mathrm{s}} = 0$ and $r_{\mathrm{s}} = 3\sigma_{\mathrm{L}}$, where $r_{\mathrm{s}} = R - \sigma$. $\tilde{f}(r)$ is computed every 10 MCS and has been averaged over 5×10^4 measures. Finally, $f(R)$ is obtained by extrapolating $\tilde{f}(r)$ for $r \rightarrow \sigma$. The protein molecules are fixed during the MC simulation and are shifted virtually only. Relaxation periods of 10^4 MCS are used when a change in the relative protein position R is performed. We have set $\delta R = 0.5$.

IV. Results and Discussion

A. Force between Conically Shaped Proteins. By using the numerical techniques described in the previous section, we have computed the force between conically-shaped proteins for the parallel and antiparallel case. The result is presented in Figure 3. In the range $r_s/\sigma_{\mathrm{L}} < 1$ one observes an attractive force which is known as the depletion-induced attraction first predicted by Asakura and Oosawa[20] and confirmed later.[21,22] The force between two colloids in a solution of lipid chains is given by

$$f(R) = MN_L\frac{\partial \ln Q}{\partial R} \tag{20}$$

$$Q = \int_V \exp[-U(\mathbf{r},R)/k_{\mathrm{B}}T]\mathrm{d}\mathbf{r} \tag{21}$$

where $U(\mathbf{r},R)$ is the interaction energy of a lipid monomer located at $\mathbf{r}$ in the presence of the two colloids separated by a distance R. Since the interaction energy is purely repulsive in our model, Q is given by the volume of space in which the lipids can move freely. One obtains Q by substracting from the total volume of the solution the volume into which the lipids cannot enter due to hindrance of the proteins, which is given by

$$Q = V - 2V_0 + v, \quad r_s/\sigma_{\mathrm{L}} < 1 \tag{22}$$

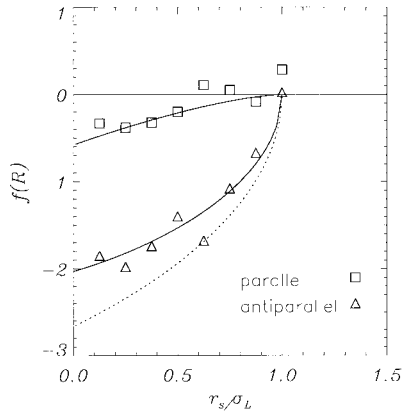

Figure 4. Comparison between theory, eqs 20 and 30 and Monte Carlo data for $f(R)$ in the range $r_s/\sigma_L < 1$. The dotted line, included for comparison, corresponds to cylindrical proteins of diameter $\sigma_P = 16$ Å, eq 31.

where $V_0 = 2/3\pi[(\sigma_P + \sigma_L)^3/8 - \sigma_L^3]H/(\sigma_P - \sigma_L)$ is the volume of one of the conically shaped proteins, including its depletion zone. $H = 40$ Å is the membrane thickness. v is the corresponding overlap between the proteins. This last term will depend on the particular protein configuration.

For the case of parallel proteins the force can be written as

$$f_{\triangledown\triangledown}(R) \sim \frac{4H}{\sigma_P - \sigma_L}\partial_R \int_{R/2}^{\sigma_0} d\sigma S(\sigma - R/2,\sigma) \qquad (23)$$

where:

$$S(x,y) = x^{3/2}({}^4/_5\sqrt{2y - x} + {}^8/_{15}\sqrt{2y}) \qquad (24)$$

defines the overlapping cross-sectional area, depending on the protein distance and height. The protein distance is $R = \sigma_P + r_s$, and

$$\sigma_0 = {}^1/_2(\sigma_P + \sigma_L) \qquad (25)$$

Due to our particular choice of the cone geometry, we have for the two inclusions

$$\sigma_h(\lambda) = \sigma_L + 2\lambda \qquad (26)$$

with $\lambda = z(\sigma_P - \sigma_L)/(2H)$.

For the antiparallel case, we have for each cone

$$\sigma_{h1}(\lambda) = \sigma_L + 2\lambda, \quad \sigma_{h2}(\lambda) = \sigma_P - 2\lambda \qquad (27)$$

thus, σ will take the following values:

$$\sigma_1(\lambda) = \sigma_L + \lambda, \quad \sigma_2(\lambda) = \sigma_0 - \lambda \qquad (28)$$

By defining the function:

$$\Upsilon(\lambda,R) = \sigma_1 - \frac{\sigma_1^2 - \sigma_2^2 + R^2}{2R} \qquad (29)$$

the force term can be written as

$$f_{\triangledown\triangle}(R) \sim \frac{4H}{\sigma_P - \sigma_L}\partial R \int_0^{(\sigma_P - \sigma_L)/2} d\lambda\, S(\Upsilon,\sigma_1) \qquad (30)$$

and $R = \sigma_0 + r_s$.

In Figure 4 we have plotted $f_{\triangledown\triangledown}(r_s)$ and $f_{\triangledown\triangle}(r_s)$ in the regime $r_s/\sigma_L < 1$ given by the full lines. The agreement between the theoretical curves and the Monte-Carlo data is reasonable. In the parallel case, where the two proteins have a very small depletion zone located near their upper part (Figure 1a), the depletion-induced attraction can be expected to be very weak which is in fact in agreement with the shallow curve in Figure 4. On the other hand, this fact might also result from a coupling effect between the upper and lower layer. While for $R = \sigma_P$, in the upper layer $r_s = 0$, and the force that acts inwards is equivalent to the osmotic presure of the lipid solution; in the lower layer $r_s = 3\sigma_L$ and such effect is negligible since the lipid density in between takes the bulk value. This is reflected in the surface density plots presented in Figure 5.

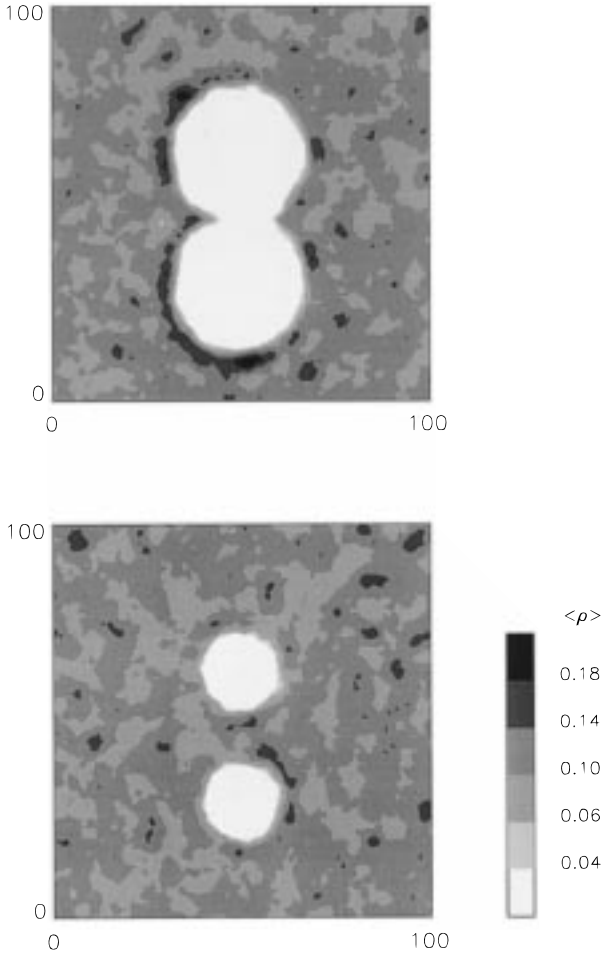

Figure 5. Contour plot of the averaged density profile per layer in the parallel configuration. The protein distance is $R = \sigma_P$. $\rho(\infty) \approx 0.1$. Top: upper layer. Bottom: lower layer.

For comparison we include in the plot a dotted line corresponding to the more simple case of two cylindrical inclusions separated a distance $R = \sigma_P + r_s$. For such protein geometry we have

$$f_{cyl}(R) \sim 2H\partial_R S(\sigma_0 - R/2,\sigma_0) \qquad (31)$$

Note that an increasing depletion zone overlap v, results in a stronger attractive force between the inclusions.

In the case of antiparallel proteins we observe a strong depletion-induced attraction at shorter distances, but also a second regime of attraction for $r_s/\sigma_L > 1.5$. These two attractive regimes are separated by a repulsive barrier. The presence of the barrier, approximately in the range $1 < r_s/\sigma_L < 1.5$ can be explained as follows. For $r_s/\sigma_L > 1$ the lipids can interfere between the two protein molecules. However, while the separation r_s is smaller than the average lipid separation in the

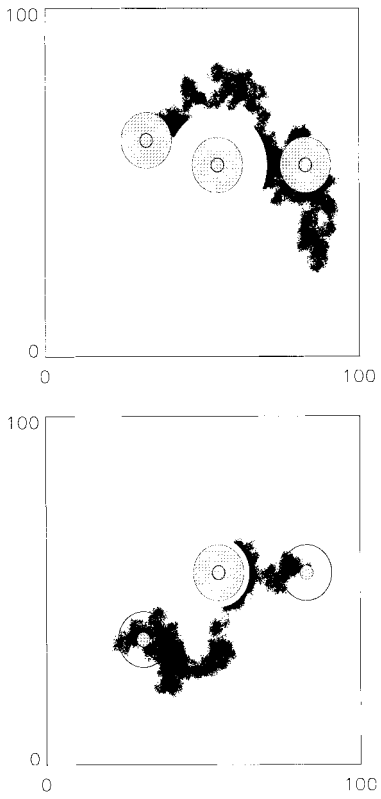

Figure 6. Diffusion of one mobile protein in the vicinity of a second immobile protein. The initial separation between surfaces is $r_s/\sigma_L = 3$. Each dot represents the center of the mobile protein at different times. Top: parallel protein configuration. Bottom: antiparallel protein configuration.

bulk, which is estimated in the model to be $r_s/\sigma_L \approx 1.7$, the lack of orientational and translational entropy result in a repulsion between them. The same packing argument may apply also for the second minima which we observe at about $r_s/\sigma_L \approx 2$. Beyond that point, the fluctuations in $f(R)$ are too large to determine its behavior and range. A possible way to examine such effect is through the study of the distortion introduced in the density and lipid order parameter field due to the presence of the proteins which is discussed in the following.

B. Fluctuation-Induced Attraction between Proteins. An evidence that a net attraction between proteins exist for $r_s/\sigma_L > 2$ can be provided by time series analysis of the interprotein distance R. In Figure 6 we present the trajectory of a protein, initially located at $r_s/\sigma_L = 3$ from a second protein that will remain immobile. We have considered both, parallel and antiparallel case. If the mobile protein is attracted by the immobile one, then the diffusional path of the mobile protein must exhibit approximately a circular trajectory around the immobile protein in the $x-y$ plane. Otherwise, in the case of vanishing attraction, the mobile protein would perform a random walk with the tendency to escape from the vicinity of the immobile protein. Every dot in Figure 6 represents the location of the center of the mobile protein at a different time and hence, the total "cloud" represents the visited area. The total run took about 10^6 Monte Carlo time steps (MCS) that we consider to be long enough to be representative of the behaviour of the system. Every 200th position is depicted the figure. The fixed protein is the one located at the center and a top view is presented.

The corresponding probability distribution $P(R)$ is plotted in Figure 7. We can observe that, in both cases, the maximum distance between the protein surfaces along the path is

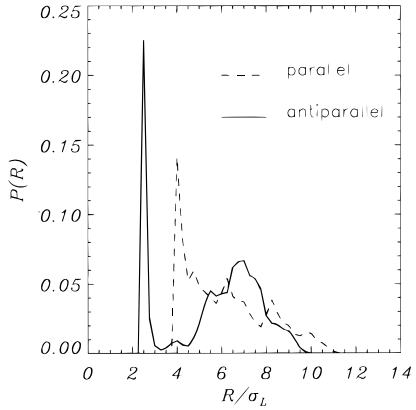

Figure 7. Probability distribution $P(R)$ of inter-protein distances. Solid and dashed lines correspond to the antiparallel and parallel protein configuration respectively.

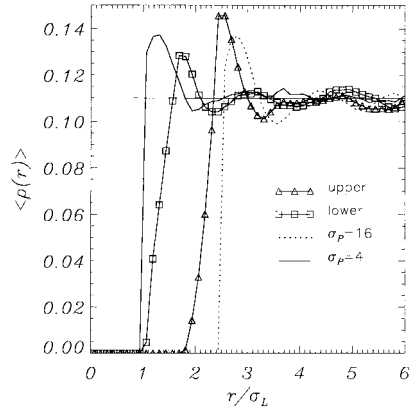

Figure 8. Density profile $\langle\rho(r)\rangle$ of lipid molecules around a conically-shaped and a cylindrical protein of diameter σ_P.

$r_s^{max}/\sigma_L \approx 6$. However, since for the antiparallel case the distribution is sharply located at $r_s = 0$, in the parallel one, a more smooth decay is observed. An estimation of the time during which the mobile protein is trapped in the depletion zone shows that in the antiparallel case it is at least 60% higher than in the parallel one.

In order to quantify the range of the long-range attractive force, we have examined in detail the perturbation in the lipid environment induced by the presence of a single protein in the membrane. We will show that the origin of the attractive force is related to the gradients of the density and orientational fluctuations of the lipids in the neighborhood of the protein. This suggestion follows the predictions from mean-field calculations[14,15] and has been already confirmed in the case of cylinder-shaped proteins.[21] Our goal is to check whether the asymmetrical geometry of proteins may affect such gradients in the case of flat bilayer membranes.

First we have considered a bilayer containing a single wedge-shaped protein which is immobile. We have analyzed the perturbation of the protein on the lower and upper lipid monolayers separately. In Figure 8 we present the density profile $\rho(r)$ of lipids around the protein,

$$\rho(r) = \sum_j \theta(r - r_j)/\pi r^2 \, dr \tag{32}$$

where the sum runs over all monomers $1 \le j \le (MN_L)$ located at distances $r_j = \sqrt{x_j^2 + y_j^2}$ with respect to the center of the protein. The θ-function is defined as $\theta(r - r_j) = 1$ if $|r - r_j| < dr = 0.5$ Å and zero otherwise. For large distances $r/\sigma_L \gg$

1 one obtains the bulk value $\langle\rho(\infty)\rangle$. At short distances $r/\sigma_L < 1$ the density decreases according to a depletion zone.[21] In Figure 8 we have also included for comparison the corresponding results in the case of proteins of cylindrical shapes, one of diameters $\sigma_P = 4$ Å and a second one of $\sigma_P = 16$ Å, where the first and the latter diameter correspond to the lower and the upper diameter of the wedge-shaped protein, respectively. According to Figure 8 the perturbations of a cylindrical and a conical protein on the lipid density $\rho(r)$ differ essentially in three points. (1) The perturbation by a cylinder is identical in the upper and the lower layer, whereas in the case of a cone the density profiles are different. (2) The change of $\rho(r)$ at short distances is almost discontinuous for a cylinder, but rather smooth for the cone. (3) Whereas the maxima of $\rho(r)$ for cylinders of various diameters are equal, the maximum in the case of a single cone is larger in the upper layer than in the lower lipid layer.

The first observation can be explained based on the different diameters of the cone-shaped protein with regard to their upper and lower part in the bilayer (compare Figure 1). The gradual increase of the diameter from the lower to the upper lipid layer must result in a different density profile as compared to case of a cylinder. For the same reason, the density profile must change gradually in accordance with the gradual change of the thickness of the cone. The third observation is probably more subtle and may have some consequences which are not very clear presently. However, it should be noted that the difference in the two maxima is significant, since this is in the order of 10%, which is much bigger than the numerical error which is comparable to size of the symbols in Figure 8. Also, the difference is too big in order to be be attributable to the different number of lipids in each of the two layers. One possible explanation could be related to the different entropies which the lipids may encounter depending on their location in proximity to the upper or lower part of the cone. Since in the upper part the tails of those lipids with their heads close to the upper edge of the cone have more space available than other lipids in the bulk, an effective force attempts to pull more lipids in this layer toward the cone. This entropy-induced attraction may result in an increased density near the cone as compared to the bulk. In the lower part of the lipid bilayer, the opposite effect may take place. There the tails of those lipids with their heads close to the lower edge of the cone have less space available than the lipids in the bulk. Therefore a repulsive force toward the bulk must be expected which may lead to a decreased local density near the cone as compared to the bulk. A possible consequence of the different density profiles in both layers would be the induction of flip-flop processes, that are not implemented in the present model, with a net amount of lipids moving from the lower to the upper layer. This effect can result in the generation of weak local curvature.

Similar observations and conclusions can also be drawn from the analysis of the average orientational profile of the lipids which is presented in Figure 9. The lipid orientational profile is calculated by

$$S(r) = \sum_j S_z(r_j)\theta(r - r_j)/\sum_j \theta(r - r_j) \tag{33}$$

where $S_z(r_j)$ is defined as

$$S_z(r_j) = {}^1/_2\langle 3[(z_{j+1} - z_j)/a_j]^2 - 1\rangle \tag{34}$$

where $\mathbf{a}_j = \mathbf{r}_{j+1} - \mathbf{r}_j$ and $z_{j+1} - z_j$ are the segmental vector and its z-component of the lipid monomer, respectively. The value for the bulk is $S(\infty) = 0.45$.

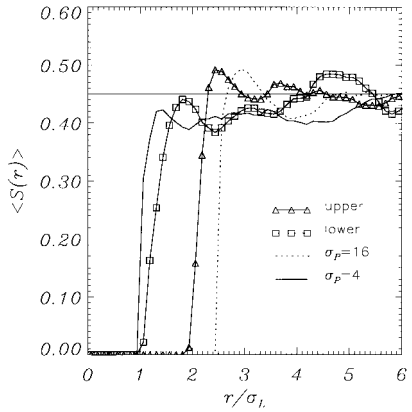

Figure 9. Lipid orientational order parameter profile $\langle S(r)\rangle$ of lipid molecules around wedge-shaped or cylindrical proteins.

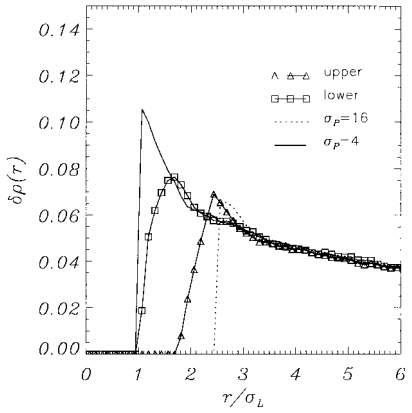

Figure 10. Density fluctuations of the mean local density of lipids $\delta\rho(r)$ around a conically-shaped protein. For comparison, lines corresponding to the inclusion of cylindrical-shaped proteins of diameter corresponding the smaller and greater cone diameter are included.

The more interesting quantities are the profiles of the density fluctuations

$$\delta\rho(r) = \sqrt{\langle[\rho(r) - \langle\rho(r)\rangle]^2\rangle} \tag{35}$$

and the orientational fluctuations

$$\delta S(r) = \sqrt{\langle[S(r) - \langle S(r)\rangle]^2\rangle} \tag{36}$$

which are shown in Figure 10 and Figure 11, respectively. A comparison between the different curves indicates that each curve can be separated in two parts: a short-range part at $\sigma_0 < r < \sigma_0 + \sigma_L$ which depends on the diameter of the cylinder or the effective diameter of the cone, and a long-range behavior at $r > \sigma_0 + \sigma_L$ which is virtually independent of the shape of the protein. In particluar, one can clearly observe that the fluctuations in the lower layer in the presence of the cone converge to the one corresponding to the presence of a cylinder with $\sigma_P = 4$ Å. The same happens in the upper layer when we compare it with a cylinder of $\sigma_P = 16$ Å. Once we exit the depletion zone area, all curves merge into a single curve independent of the shape or diameter of the protein. The same effect is observed with the orientational fluctuation (Figure 11). The long-range behavior may be interpreted as evidence for the existence of a universal behavior of $\delta\rho(r)$. The fluctuations decrease with increasing distance from the protein and settle to some constant value characteristic of the bulk: $\delta\rho(\infty) \approx 0.03$

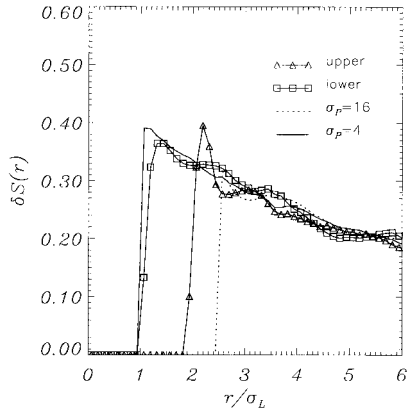

Figure 11. Same as Figure 10 for the local orientational fluctuations $\delta S(r)$.

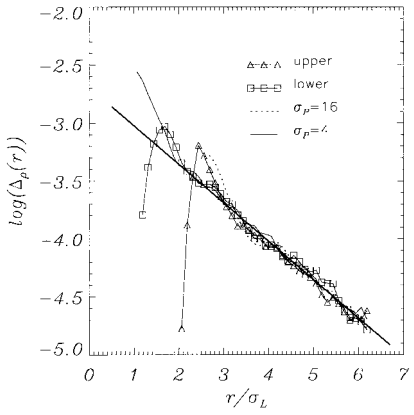

Figure 12. Semilog plot of the fluctuations $\Delta_\rho(r) = \delta\rho(r) - \delta\rho(\infty)$ for $r/\sigma_L > 1$.

and $\delta S(\infty) \approx 0.2$. A semilog arithmic plot presented in Figure 12 of the density fluctuations indicate an exponential decay according to

$$\delta S(r) - \delta S(\infty) \sim \exp(-r/\xi) \tag{37}$$

where $\xi/\sigma_L \approx 3.0$. This is in qualitative agreement with earlier mean-field calculations[15,17] which yield

$$\delta S(r) - \delta S(\infty) \sim K_o(r/\xi) \tag{38}$$

where $K_o(x)$ is the modified Bessel function with the limiting behavior $K_o(x) \sim \exp(-x)/\sqrt{x}$ for $x \rightarrow \infty$. Whereas the $\langle\rho(r)\rangle$ decays rapidly to $\rho(\infty)$, the corresponding fluctuations $\langle\delta\rho(r)\rangle$ is long-ranged. Thus, it indicates that, in regions where modified lipid fluctuations overlap, a lipid mediated attraction between proteins takes place. This suggestion is in agreement with the conclusions of Schröder's work[15] based on linear response theory.

Our results show that stretched planar membranes, and in a distance of a few lipid layers ($r_s/\sigma_L \approx 6$) an attractive interaction wich originates on density and orientational fluctuations takes place. Such interaction is independent of the protein size and protein-boundary shape, and appears to be a universal type of behavior in the range described.

V. Summary and Conclusions

We have reported extensively Monte Carlo simulations on a lipid bilayer membrane containing two cone-shaped proteins. We have studied the protein interaction for parallel and antiparallel configurations of two cone-shaped proteins. We have neglected effects due to undulations and bending stiffness thus, the membrane has zero spontaneous curvature. We have focused on effects related to the fluctuations of the lipid orientational order and lipid density in the vicinity of a protein. We found two types of attraction with different regimes. A depletion-induced attraction in the range $r_s < \sigma_L$, where σ_L is the diameter of a lipid and r_s is the distance between the surfaces of the two proteins. This result is consistent with the Asakura−Oosawa approximation.

In the range $1 < r_s/\sigma_L < 6$ we observe a fluctuation-induced attraction which originates from the overlap of the gradients of density and orientational fluctuations of the lipids around each protein. This interaction is shown to be independent of the relative protein configuration (i.e., parallel or antiparallel) and independent of the shape and size of the proteins. In this regime, the fluctuations behave similar as in the case of symmetric inclusions respect to the middle plane separating the layers, with the same correlation length. Since the attraction is found to be protein shape independent, it may depend on the lipid model. We expect that in a more realistic model for the lipid chain, including higher degrees of freedom, the constrains imposed on the lipid structure because of the presence of a nearby protein are going to be more important. A higher lack of entropy may be traduced in a more attractive potential well.

Possible extensions of the present work may include local curvature effects and membrane shape undulations.

Acknowledgment. Financial support of T.S. by the Commission of the European Communities (Marie Curie Fellowship ERBFMBICT961451) is gratefully acknowledged.

References and Notes

(1) Darnel, J.; Lodish, H.; Baltimore, D. *Molecular Cell Biology*; Scienfic American: New York, 1986.

(2) Bloom, M.; Evans, E.; Mouritsen, O. G. *Q. Rev. Biophys.* **1991**, *24*, 293.

(3) Warren, G. B.; Toon, P. A.; Birdsall, N. J.; Lee, A. G.; Metcalfe, J. C. *Biochemistry* **1974**, *13*, 5501.

(4) Kleeman, W.; McConnell, H. M. *Biochim. Biophys. Acta* **1974**, *345*, 220.

(5) Israelachvili, J. *Intermolecular and Surface Forces, 2nd Ed.*; Academic Press: London, 1992.

(6) Mouritsen, O. G.; Bloom, M. *Annu. Rev. Biophys. Biomol. Struct.* **1993**, *22*, 145.

(7) Ben-Tal, N.; Honig. B. *Biophys. J.* **1996**, *71*, 3046.

(8) Gruler, H.; Sackmann, E. *Croat. Chem. Acta* **1977**, *49*, 379.

(9) Goulian, M.; Bruinsma, R.; Pincus, P. *Europhys. Lett.* **1993**, *22*, 145.

(10) Dan, N.; Berman, A.; Pincus, P.; Safran, S. A. *J. Phys. II* **1994**, *4*, 1713.

(11) Park, J.-M.; Lubensky, T. C. *J. Phys. I* **1996**, *6*, 1217.

(12) Golestanian, R.; Goulian, M.; Kardar, M. *Europhys. Lett.* **1996**, *33*, 241.

(13) Aranda-Espinoza, H.; Berman, A.; Dan, N.; Pincus, P.; Safran, S. *Biophys. J.* **1996**, *71*, 648.

(14) Marčelja, S. *Biochim. Biophys. Acta* **1976**, *455*, 1.

(15) Schröder, H. *J. Chem. Phys.* **1977**, *67*, 1617.

(16) Owicki, J. C.; McConnell, H. M. *Proc. Natl. Acad. Sci. U.S.A.* **1979**, *76*, 4750.

(17) Pearson, T. L.; Edelman, J.; Chan, S. I. *Biophys. J.* **1984**, *45*, 863.

(18) Odell, E.; Oster, G. *Lect. Math. Life Sci.* **1994**, *24*, 23.

(19) Dan, N.; Pincus, P.; Safran, S. A. *Langmuir* **1993**, *9*, 2768.

(20) Asakura, S.; Oosawa, F. *J. Chem. Phys.* **1954**, *22*, 1255. *J. Polym. Sci.* **1958**, *33*, 183.

(21) Sintes, T.; Baumgaertner, A. *Biophys. J.* **1997**, *73*, 2251.

(22) Ohshima, Y. N.; Sakagami, H.; Okumoto, K.; Tokoyoda, A.; Igarashi, T.; Shintaku, K. B.; Toride, S.; Sekino, H.; Kabuto, K.; Nishio, I. *Phys. Rev. Lett.* **1997**, *78*, 3963.

(23) Möhwald, H. *Ann. Rev. Phys. Chem.* **1990**, *41*, 441.

(24) Haas, F. M.; Hilfer, R.; Binder, K. *J. Chem. Phys.* **1995**, *102*, 2960.
(25) Xiang, T.-X. *Biophys. J.* **1995**, *65*, 1108.
(26) Baumgaertner, A. *J. Chem. Phys*. **1995**, *103*, 10669.
(27) Allen, M.; Tildesley, D. *Computer Simulation of Liquids*; Clarendon: Oxford, 1987.
(28) Gennis, R. B. *Biomembranes: Molecular Structure and Function*; Springer: New York, 1989.
(29) Dickman, R.; Yethiraj, A. *J. Chem. Phys*. **1994**, *100*, 4683.
(30) Toral, R.; Chakrabarti, A.; Dickman, R. *Phys. Rev. E* **1994**, *50*, 343.